JARO: 161–176 (2021)
DOI: 10.1007/s10162-021-00785-4

JARO
Journal of the Association for Research in Otolaryngology

Research Article

Residual Hair Cell Responses in Electric-Acoustic Stimulation Cochlear Implant Users with Complete Loss of Acoustic Hearing After Implantation

Viral D. Tejani,[1,2] Jeong-Seo Kim,[1,2] Jacob J. Oleson,[3] Paul J. Abbas,[1,2] Carolyn J. Brown,[1,2] Marlan R. Hansen,[1,4] and Bruce J. Gantz[1,4]

[1]*Department of Otolaryngology-Head and Neck Surgery, University of Iowa Hospitals and Clinics, Iowa City, IA, USA*

[2]*Department of Communication Sciences and Disorders, University of Iowa, Iowa City, IA, USA*

[3]*Department of Biostatistics, University of Iowa, Iowa City, IA, USA*

[4]*Department of Neurosurgery, University of Iowa Hospitals and Clinics, Iowa City, IA, USA*

Received: 14 October 2020; Accepted: 3 January 2021; Online publication: 4 February 2021

ABSTRACT

Changes in cochlear implant (CI) design and surgical techniques have enabled the preservation of residual acoustic hearing in the implanted ear. While most Nucleus Hybrid L24 CI users retain significant acoustic hearing years after surgery, 6–17 % experience a complete loss of acoustic hearing (Roland et al. Laryngoscope. 126(1):175-81. (2016), Laryngoscope. 128(8):1939-1945 (2018); Scheperle et al. Hear Res. 350:45-57 (2017)). Electrocochleography (ECoG) enables non-invasive monitoring of peripheral auditory function and may provide insight into the pathophysiology of hearing loss. The ECoG response is evoked using an acoustic stimulus and includes contributions from the hair cells (cochlear microphonic—CM) as well as the auditory nerve (auditory nerve neurophonic—ANN). Seven Hybrid L24 CI users with complete loss of residual hearing months after surgery underwent ECoG measures before and after loss of hearing. While significant reductions in CMs were evident after hearing loss, all participants had measurable CMs despite having no measurable acoustic hearing. None retained measurable ANNs. Given histological data suggesting stable hair cell and neural counts after hearing loss (e.g., Quesnel et al. Hear Res. 333:225-234. (2016)), the loss of ECoG and audiometric hearing may reflect reduced synaptic input. This is consistent with the theory that residual CM responses coupled with little to no ANN responses reflect a "disconnect" between hair cells and auditory nerve fibers (Fontenot et al. Ear Hear. 40(3):577-591. 2019). This "disconnection" may prevent proper encoding of auditory stimulation at higher auditory pathways, leading to a lack of audiometric responses, even in the presence of viable cochlear hair cells.

Keywords: electrocochleography, hearing preservation, electric-acoustic stimulation, hybrid, cochlear microphonic, auditory nerve neurophonic

INTRODUCTION

Cochlear implant (CI) electrode array designs and surgical techniques have evolved such that preserving residual acoustic hearing is likely after surgery. This allows for combined electric and acoustic stimulation (EAS) in the implanted ear, where a hearing aid and a CI are integrated to provide low-frequency acoustic amplification and high-frequency electrical stimulation, respectively. EAS CI users achieve better speech understanding abilities relative to electric-only hearing (Helbig et al. 2011; Lenarz et al. 2013; Gantz et al. 2016, 2018; Roland et al. 2016, 2018; Pillsbury et al. 2018). EAS CI users implanted with the Nucleus L24 Hybrid CI maintain stable low-frequency audiometric thresholds (125, 250, and 500 Hz) of 50–70 dB HL up

Correspondence to: Viral D. Tejani · Department of Communication Sciences and Disorders · University of Iowa · Iowa City, IA, USA. email: viral-tejani@uiowa.edu

to 5 years after implantation (Gantz et al. 2018; Roland Jr et al. 2018). However, 6–17 % experience total loss of acoustic hearing several months after surgery (Roland et al. 2016, 2018; Scheperle et al. 2017). *Total loss* is defined as no audiometric responses from 125–8000 Hz. Regardless of electrode manufacturer and length, a *partial loss* up to 30 dB immediately and/or several months after surgery is expected in 30–40 % of patients. This loss, however, does not preclude use of acoustic amplification (Lenarz et al. 2013; Van Abel et al. 2015; Scheperle et al. 2017; Pillsbury et al. 2018; Roland Jr et al. 2018).

Initial loss of hearing is attributed to structural trauma to the cochlea (e.g. Adunka et al. 2010). However, the pathophysiology of "delayed-onset" hearing loss is unknown, though there are several theories. For example, changes in intracochlear electrode impedances may reflect changes in the cochlear tissue environment (Choi et al. 2017; Scheperle et al. 2017) such as a fibrotic reaction to the electrode array (O'Leary et al. 2013; Tanaka et al. 2014; Quesnel et al. 2016; Foggia et al. 2019). The lateral wall placement of some hearing preservation arrays may cause trauma to the stria vascularis, compromising cochlear blood supply and endocochlear potential, and resulting in high-frequency hearing loss where the electrode resides. However, stria damage is not associated with delayed low-frequency hearing loss (Tanaka et al. 2014; Reiss et al. 2015). Histological analysis indicates stable hair cell/spiral ganglion neuron counts at all frequency regions for implanted ears and non-implanted controls (O'Leary et al. 2013; Tanaka et al. 2014; Reiss et al. 2015; Quesnel et al. 2016). This suggests alternative mechanisms such as compromised endocochlear potential (Tanaka et al. 2014; Reiss et al. 2015), changes in cochlear mechanics due to intracochlear fibrosis (Choi and Oghalai 2005), or other structural pathologies not visibly detected. The stable hair cell/neural counts are also consistent with our previous report of stable electrically evoked compound action potentials (ECAPs) before and after loss of acoustic hearing (Scheperle et al. 2017). ECAPs are a direct measure of neural activity in response to electrical stimulation, bypassing the hair cells and synapse. The stable hair cell/neural counts and stable ECAPs are consistent with the hypothesis of cochlear neuropathy/synaptopathy following CI (Kopelovich et al. 2015; Li et al. 2020).

Our lab has used electrocochleography (ECoG) as an objective electrophysiological tool to monitor peripheral auditory function over time in Hybrid CI users (Abbas et al. 2017; Kim et al. 2018; Tejani et al. 2019; see Eggermont 2017 for review on ECoG). The electrocochleogram consists of hair cell and neural potentials. The cochlear microphonic (CM) is a hair cell response that mimics the stimulus. The compound action potential (CAP) is a neural response occurring at the stimulus onset and offset, while the auditory nerve neurophonic (ANN) is a sustained phase-locked neural response. The summating potential (SP) presents as a baseline shift and may contain both hair cell and neural contributions (Pappa et al. 2019). CM and ANN response thresholds and amplitudes are stable for Hybrid CI users with stable hearing, while declines in response thresholds correlate with declines in audiometric hearing, validating ECoG as a longitudinal objective marker of peripheral auditory function (Abbas et al. 2017; Kim et al. 2018; Tejani et al. 2019). Our previous report also showed one Hybrid CI user who had reduced, but still present, CM responses at 14 months after surgery, despite total loss of audiometric acoustic hearing (subject L22R of Abbas et al. 2017).

The purpose of this study was to determine the presence/absence of CM and ANN responses in L24 Hybrid CI users who demonstrated total loss of residual acoustic hearing. If these Hybrid CI users also show residual hair cell function (CM) but no neural function (ANN) (as in subject L22R), this may provide insight into the pathophysiology of delayed-onset hearing loss and inform future medical therapies.

METHODS

Subjects

Data from seven L24 Hybrid CI users were obtained retrospectively from previous studies in our lab (Abbas et al. 2017; Kim et al. 2018; Tejani et al. 2019) or were collected prospectively. The L24 Hybrid CI is a 22-electrode array that has a shallow insertion depth (16 mm) and is approved by the Food and Drug Administration for hearing preservation (Lenarz et al. 2013; Roland et al. 2016, 2018). These seven study participants were part of a larger cohort implanted by authors BJG and MRH at University of Iowa Hospitals and Clinics using hearing preservation protocols. Hybrid candidacy guidelines included pre-operative audiometric thresholds $\leq$ 60 dB HL at 125–500 Hz and a high-frequency pure-tone average (PTA, 2000–4000 Hz) $\geq$ 75 dB HL in the ear to be implanted. These subjects were selected from our entire cohort as they initially had low-frequency hearing preserved in the implanted ear post-operatively, but later experienced total loss of acoustic hearing (audiometric thresholds > 115 dB HL at all frequencies 125–8000 Hz). Additionally, they had ECoG testing done before and after loss of acoustic hearing. The time point of total hearing loss averaged at 9.15 ± 5.03 months after activation of the CI. Table 1 indicates

TABLE 1

Subject demographics, including age, pre-operative low-frequency PTA, and time point of total hearing loss

Subject ID	*Gender*	*Pre-operative pure-tone average (125–500 Hz) (dB HL)*	*Date of initial activation*	*Age at initial activation (years)*	*Onset of total hearing loss (months after initial activation)*
L22R	F	27	8/5/2014	48	12.49
L32R	F	22	5/24/2014	60	15.89
L54R	F	40	9/23/2016	75	11.18
L55R	M	50	9/13/2015	74	2.84
L62L	M	50	3/2/2017	71	3.46
L66R	M	40	5/17/2017	77	12.16
L81R	F	27	7/11/2018	68	6

Subject Demographics

subject demographics, including age, pre-operative low-frequency PTA, and time point of total hearing loss. This study was approved by the University of Iowa Institutional Review Board. All subjects signed an informed consent form.

Electrocochleography Recordings

Low-frequency tone bursts were presented to the implanted ear via an insert earphone using both condensation and rarefaction polarities. Stimuli frequencies were 250, 500, 750, and 1000 Hz presented at a 10-Hz stimulation rate. Presentation levels varied from below behavioral detection threshold to the maximal comfort level. An adaptation of the Neural Response Telemetry (NRT) system contained within Custom Sound EP was utilized to record responses from the most apical electrode in the electrode array. While the NRT system is normally used to record *electrically* evoked auditory potentials, the software was adapted to trigger an external *acoustic* stimulus generator. The trigger pulse synchronized the onset of stimulus generation with the onset of the recording of the intracochlear acoustic response. For more details regarding the software adaptation, see Abbas et al. (2017), Kim et al. (2018), and Tejani et al. (2019).

In all cases, a control recording was performed to rule out transducer-related stimulus artifacts. To obtain this recording, the stimulus was played at a high intensity, but the insert earphone was removed from the subject's ear canal, with the transducer remaining on the subject's shoulder. The recorded response should only reflect system noise floor and artifacts related to switching on the internal NRT recording amplifier. If there was also a transducer-related stimulus artifact, the control recording waveform would look like a CM or ANN response. There was no evidence of transducer-related stimulus artifacts in the control recording waveforms.

Recordings were repeated at several time points after activation of the CI. These time points typically coincided with their clinical checkup appointments, and included 0.5, 1, 3, 6, and 12 months, as well as annually after 12 months. Exact time points varied based on study participants' availability. Participants were also seen for interim appointments if they experienced a loss of acoustic hearing. Additionally, while recordings were attempted for all stimulus frequencies, we initially focused on 500 Hz due to time/equipment limitations early in the experimental protocol. For recent recordings, we were able to record responses to all four stimulus frequencies (250, 500, 750, and 1000 Hz).

Electrocochleography Analysis

Each ECoG recording consisted of an average of 100–400 sweeps. Responses to condensation and rarefaction stimuli were subtracted from one another to emphasize the CM and added to emphasize the ANN (Aran and Charlet de Sauvage 1976; Henry 1995; Lichtenhan et al. 2013). Recognizing that the difference and summation technique does not result in a pure separation of CM and ANN (Forgues et al. 2014; Abbas et al. 2017), we refer to the difference potentials as CM/DIF and the summed potentials as ANN/SUM for the remainder of this report.

Figure 1 shows an exemplar waveform from subject L81R tested at 0.5 months after activation of her CI. The left panel shows the individual rarefaction and condensation polarities in response to a 500-Hz stimulus presented at 108 dB SPL. The middle and right panels show the CM/DIF and ANN/SUM potentials. Note that the CM/DIF oscillates at the stimulus frequency while the ANN/SUM oscillates at twice the stimulus frequency. ECoG amplitudes were quantified as the difference in amplitude of the trough and following peak of the time waveform over one cycle (black circles in middle and right panels; corresponding amplitudes shown in the upper-right-hand corner of each panel). The cycle that was chosen was located in the middle, steady-state, portion of the response waveform. We chose the middle portion of the response waveform to avoid any onset/offset response that could confound the true

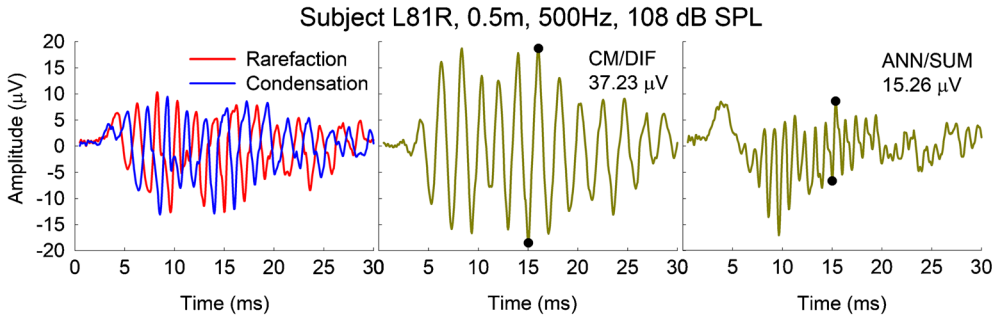

FIG. 1. The left panel shows responses to a 500-Hz stimulus presented in rarefaction and condensation polarities. The middle and right panels show the resulting CM/DIF and ANN/SUM responses, with their corresponding amplitudes indicated in the upper-right-hand corner of each panel. The locations of the trough and peak used to determine the amplitude are indicated by the filled black circles

CM/ANN amplitude (e.g., Fontenot et al. 2019). Amplitudes were considered present if they were above the recording noise floor. The noise floor was obtained from the previously described control recordings. The noise floor was 1.73 μV, which represents an average of noise floors across all seven subjects (standard deviation = 0.70 μV).

RESULTS

While all subjects had preserved CM/DIF and ANN/SUM responses following cochlear implantation, we found total loss of ANN/SUM potentials in all seven patients following total hearing loss. Figure 2 shows the CM/DIF and ANN/SUM potentials for all subjects in response to a 500-Hz stimulus before and after total loss of hearing. Despite the higher stimulus levels used after hearing loss (105–115 dB SPL), there is no ANN/SUM response after hearing loss while the CM/DIF response is still present, albeit at a reduced amplitude. As the previously performed control recordings contained no stimulus-related artifacts, the experimental ECoG responses were judged to be valid and not compromised by stimulus artifacts.

Figure 3 shows a summary of longitudinal ECoG data collected from subject L32R. The left panel shows serial audiograms obtained between 2 weeks and 4 years after activation of her CI. The middle and right panels show CM/DIF and ANN/SUM amplitude growth functions, respectively, in response to 250, 500, 750, and 1000 Hz stimuli. These growth functions were obtained at the same time as audiometric testing and show growth of CM/DIF and ANN/SUM responses as the stimulation level increases.

As shown on the left panel of Fig. 3, L32R had successful preservation of low-frequency hearing for the first 10 months of CI use. A few months afterwards, she experienced a substantial decline in hearing. Steroids were prescribed, resulting in some transient improvement in her 500 Hz audiometric threshold between 16 and 17 months. Ultimately, steroids were not successful in maintaining her hearing, and at 20 months after CI, her audiogram indicated a profound hearing loss at all frequencies (audiogram not shown in the figure). At 48 months, her audiogram continued to confirm a profound hearing loss. Focusing on the 500 Hz ECoG amplitude growth data, CM/DIF and ANN/SUM responses collected prior to loss of hearing (0.5, 3, 6, and 10 months) show relatively stable amplitudes. At 16 and 17 months, higher stimulation levels were required to evoke CM/DIF and ANN/SUM potentials, consistent with her partial loss of acoustic hearing. In addition, note that at 17 months, there is a transient improvement in her 500 Hz ECoG amplitudes compared to her 16-month appointment, reflective of the transient improvement in her 500-Hz audiometric threshold. Specifically, there was no ANN/SUM response at 16 months, while at 17 months, a response was present. ECoG testing was not completed at her 20-month post-activation visit, but at 48 months, despite the total loss of acoustic hearing, CM/DIF potentials were recordable with amplitudes of 10–20 μV (well above the noise floor, albeit still reduced compared to pre-hearing loss amplitudes), while ANN/SUM potentials were not.

As another example, Fig. 4 shows longitudinal audiograms, CM/DIF, and ANN/SUM amplitude growth functions for subject L22R. At 12 months, she experienced significant hearing loss, which led to a partial reduction in 500 Hz CM/DIF responses and a complete reduction in 500 Hz ANN/SUM responses. Steroids partially reversed her hearing loss, and at 12.1 months, she showed improved audiometric thresholds, CM/DIF responses, and ANN/SUM responses. However, she experienced total loss of acoustic hearing shortly afterwards. Despite the complete loss of acoustic hearing, CM/DIF responses at amplitudes of 10 μV were still present at 60 months

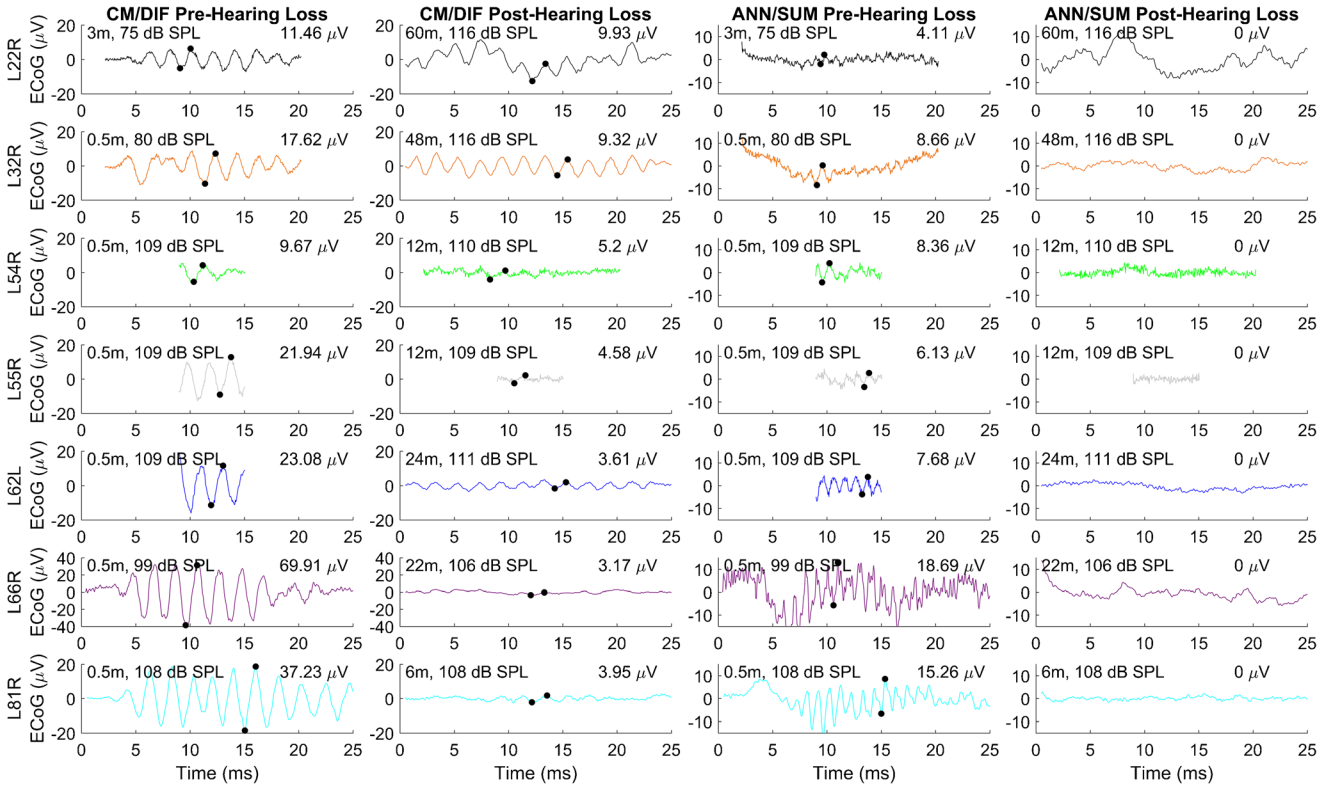

FIG. 2. The left two columns show CM/DIF responses to a 500-Hz stimulus prior to and after total loss of acoustic hearing. The right two columns show the ANN/SUM responses prior to and after total loss of acoustic hearing. Each row represents one subject. Response amplitudes are indicated in the upper-right corner of each panel. Test session in months and stimulation levels in dB SPL are indicated in the upper-left corner of each panel. The locations of the trough and peak used to determine the amplitude are indicated by the filled black circles. There was no evidence of an ANN/SUM response after hearing loss, despite the higher stimulation levels used

after CI activation, while there was no evidence of ANN/SUM responses.

Data for five other patients who also had total loss of acoustic hearing are shown as Figs. 5, 6, 7, 8, and 9. In all cases, CM/DIF and ANN/SUM responses were present before loss of acoustic hearing. Similarly, after total loss of acoustic hearing, CM/DIF responses were present, but at reduced amplitudes, while ANN/SUM responses were absent.

Figure 10 summarizes audiometric and ECoG data collected for 500 Hz stimulation for all subjects, as the greatest amount of data was available at this frequency. Specifically, we focus on data collected at one time point before and one time point after total loss of hearing, as specified by the table in the upper-left-hand corner of Fig. 10. Figure 10A shows the total loss of audiometric hearing at 500 Hz. Figure 10B and C show CM/DIF amplitude growth functions before and after hearing loss. After total loss of hearing, it is clear that CM/DIF responses are still present, but at substantially reduced amplitudes ($\leq$ 10 μV) and that higher stimulation levels are required to evoke the CM/DIF responses. Figure 10D and E show the presence and absence of ANN/SUM responses before and after hearing loss, respectively, for all seven subjects.

The results presented in Fig. 10 suggest both CM/DIF and ANN/SUM response are reduced after total loss of hearing. More specifically, in no cases were ANN/SUM responses present after total loss of hearing. One caveat is that for a given stimulus level, the resulting ANN/SUM responses are smaller than CM/DIF responses and closer to the noise floor (Forgues et al. 2014; Abbas et al. 2017; Koka et al. 2017; Kim et al. 2018; Tejani et al. 2019). Thus, the noise floor may obscure any true residual ANN/SUM responses after total loss of acoustic hearing.

To address this concern, we extracted ECoG data from 51 L24 Hybrid CI users in our research database to build a model and form a prediction of the ANN/SUM amplitudes given a set of CM/DIF amplitudes. We reasoned that since the ANN/SUM grows with the CM/DIF as the stimulus level increases (e.g., Figs. 3, 4, 5, 6, 7, 8, 9, and 10), we can model the growth of the ANN/SUM based on the growth of the CM/DIF. Based on this model, we then formed a prediction interval of the expected ANN/SUM amplitude given the CM/DIF

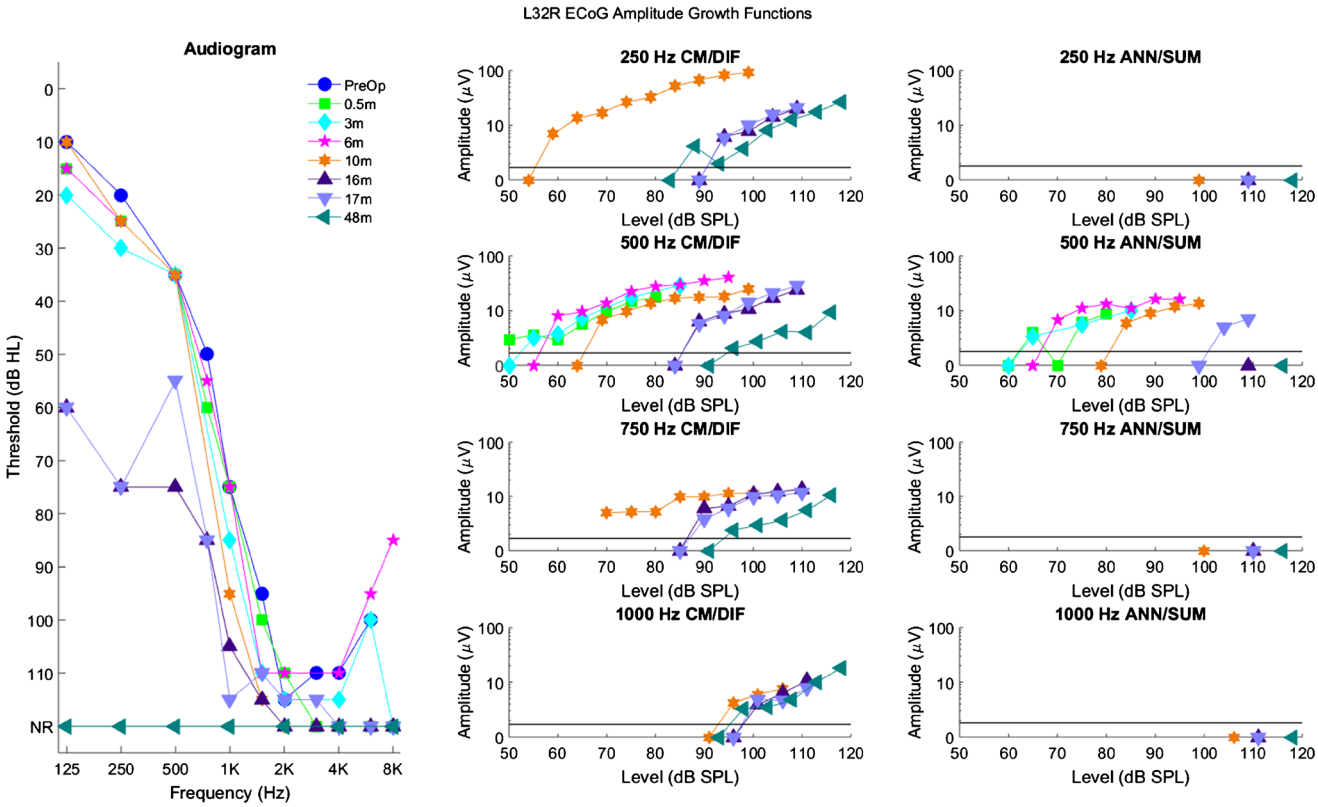

FIG. 3. Longitudinal audiograms and ECoG amplitude growth functions for subject L32R. The left panel shows serial audiograms from the pre-operative period to 48 months after activation of the CI (NR indicates no response at the limits of the audiometer). The middle and right columns show CM/DIF and ANN/SUM amplitude growth functions for the corresponding time points. The solid line at 1.73 μV represents the noise floor. Each row represents a different frequency from 250 to 1000 Hz. Note that before loss of hearing, CM/DIF and ANN/SUM responses were present. After loss of hearing, only CM/DIF responses were present, but at reduced amplitudes, while ANN/SUM amplitudes were absent

amplitudes in our seven subjects after total loss of acoustic hearing.

All 51 subjects used to build the model had measurable acoustic hearing, as well as measurable CM/DIF and ANN/SUM potentials. The subject set did not include the seven subjects of the current study. Figure 11 exemplifies how one subject was used to build the model. ECoG amplitude growth functions were obtained (Fig. 11, left panel). Subsequently, the CM/DIF and the corresponding ANN/SUM potentials were plotted against one another (Fig. 11, right panel). Cases of no responses (0 μV amplitudes) were excluded to avoid the aforementioned noise floor issue.

Figure 12 shows CM/DIF as well as the corresponding ANN/SUM amplitudes for all 51 subjects. The ANN/SUM amplitude increases with CM/DIF amplitude, which was verified by a linear mixed-effects regression model. The outcome variable was the ANN/SUM amplitude, the fixed effect was the CM/DIF amplitude, and a random intercept for subjects was included to account for the repeated observations per subject as well as a random slope for CM/DIF. The model was fit using SAS v9.4 with REML estimates provided. The linear mixed-effects model verified that an increase in CM/DIF was significantly related to an increase in ANN/SUM (beta = 0.215, $t_{32} = 6.39$, $p < 0.0001$).

As a validation measure, the CM/DIF amplitudes *before hearing loss* (Fig. 10B) were used as inputs to the linear mixed-effects model to form a prediction interval of the expected ANN/SUM amplitude based on the CM/DIF amplitude. Figure 13 shows the predicted and measured ANN/SUM amplitudes before hearing loss based on the measured CM/DIF amplitude before hearing loss. The filled data points represent the ANN/SUM amplitude growth functions (same data as Fig. 10D), while the open symbols represent the predicted ANN/SUM ± 95 % prediction interval. The predicted ANN/SUM amplitude in most cases overlaps with the measured ANN/SUM amplitude, indicating how well the model fits the new data.

Note that the prediction intervals tend to be wider for the larger ANN/SUM amplitudes, due to the

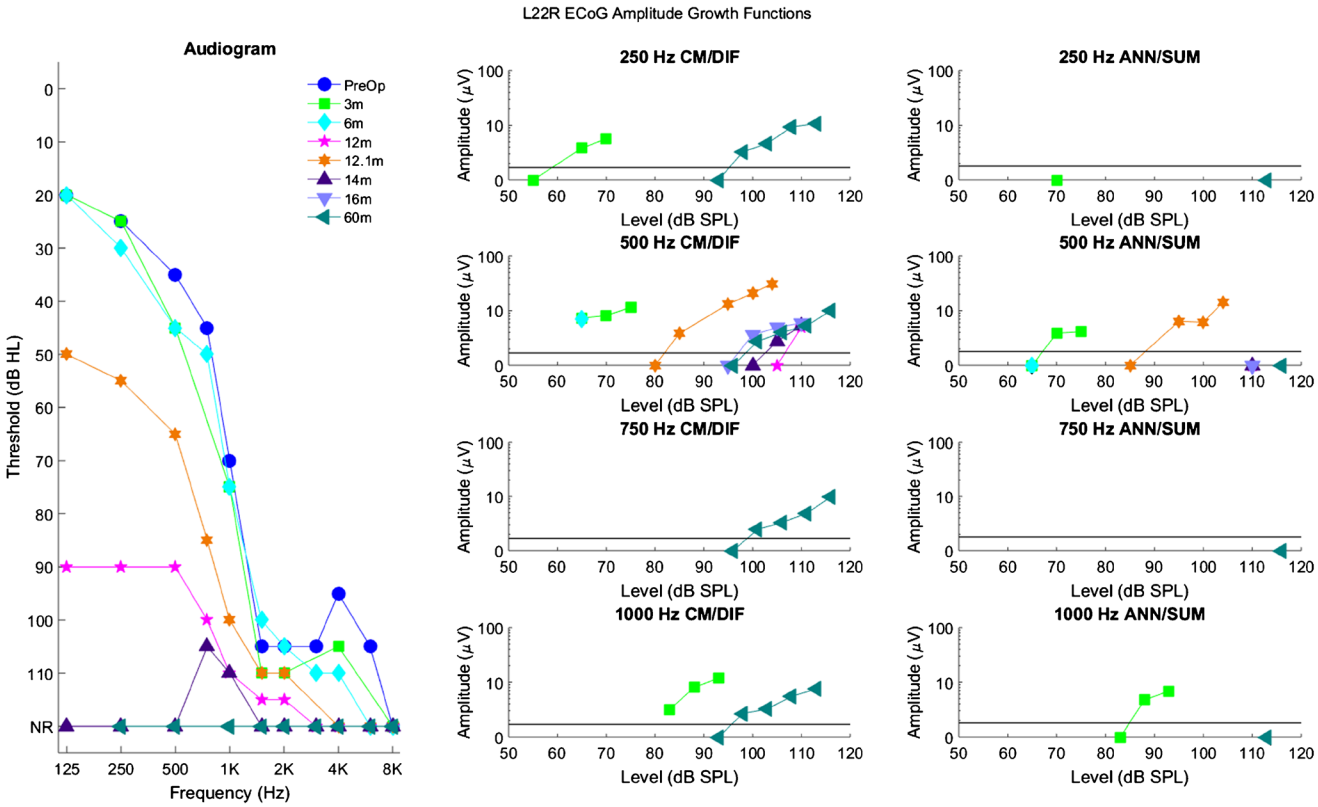

FIG. 4. Longitudinal audiograms and ECoG amplitude growth functions for subject L22R up to 60 months after activation of the CI. Details of the figure are otherwise the same as those of Fig. 3

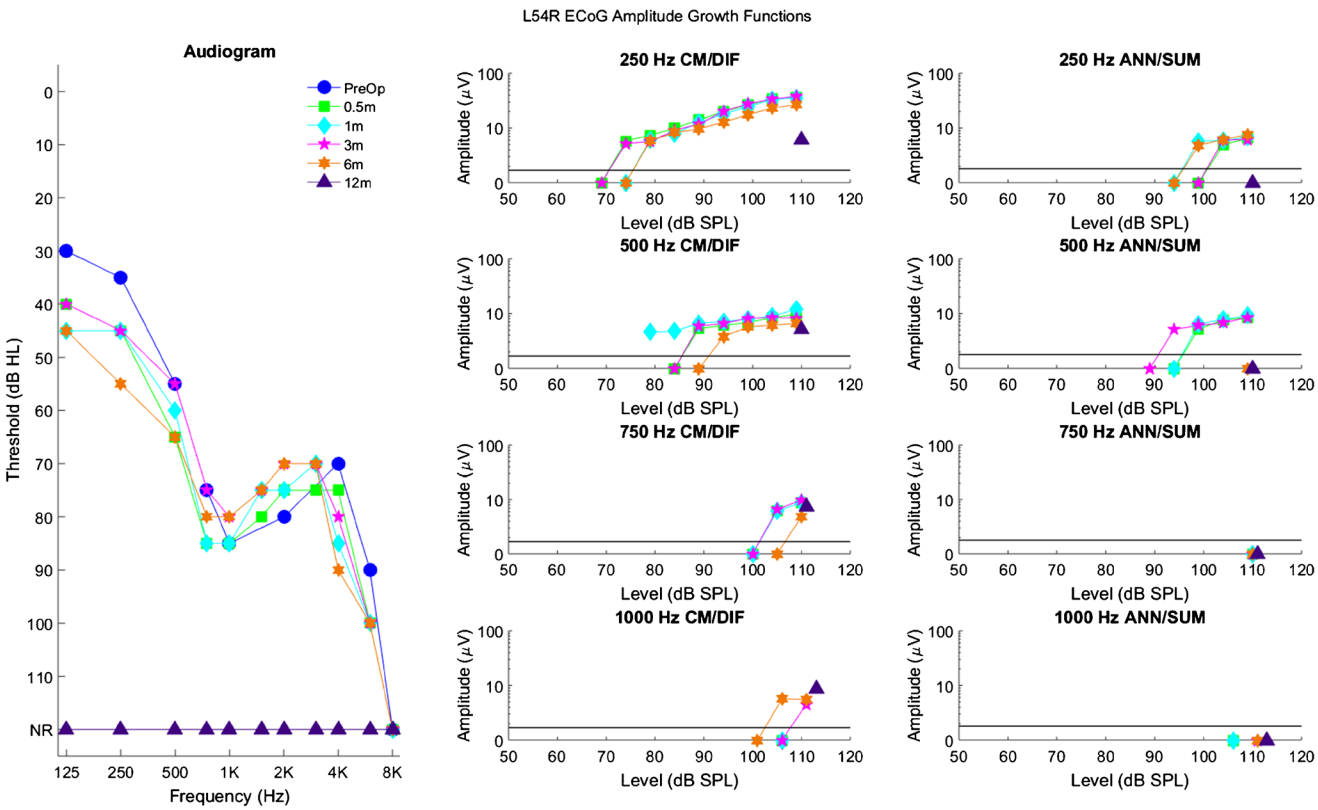

FIG. 5. Longitudinal audiograms and ECoG amplitude growth functions for subject L54R up to 12 months after activation of the CI. Details of the figure are otherwise the same as those of Fig. 3

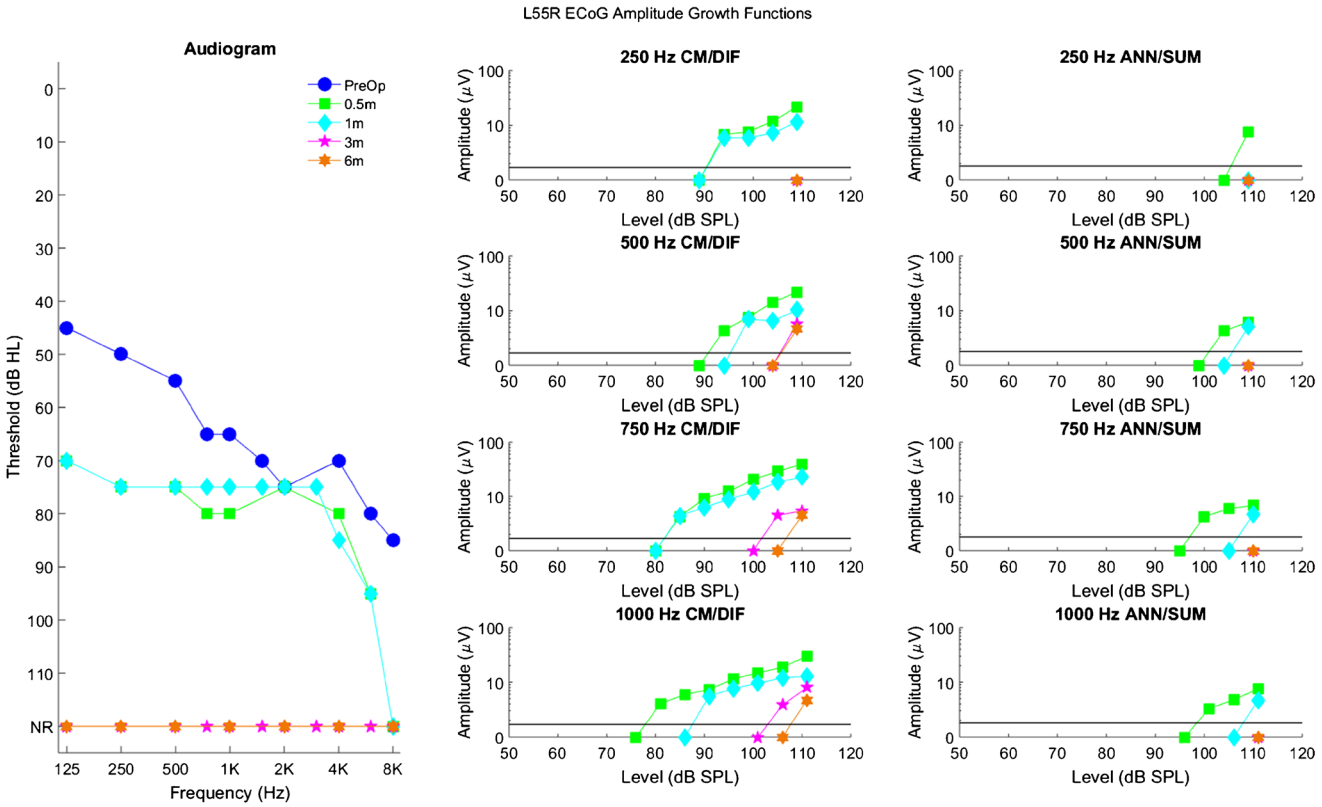

FIG. 6. Longitudinal audiograms and ECoG amplitude growth functions for subject L55R up to 6 months after activation of the CI. Details of the figure are otherwise the same as those of Fig. 3

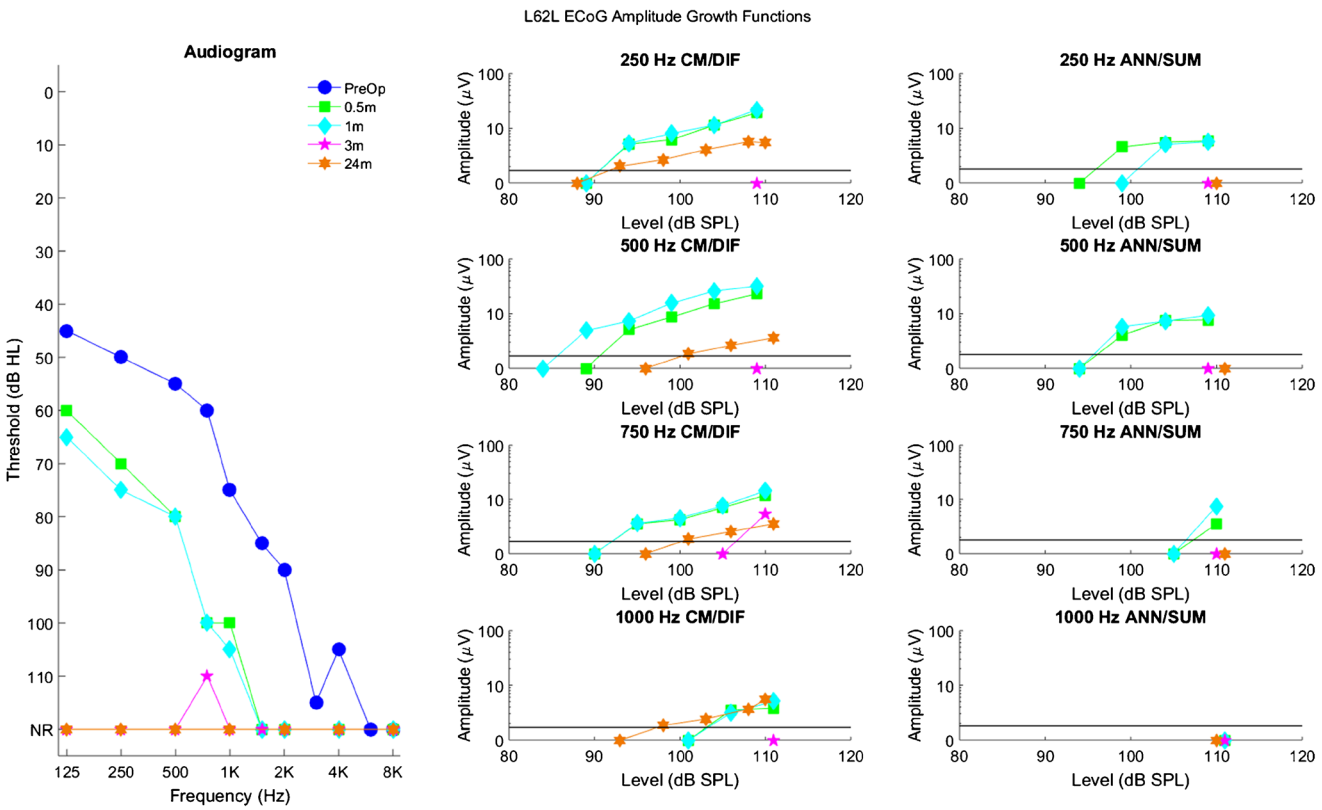

FIG. 7. Longitudinal audiograms and ECoG amplitude growth functions for subject L62L up to 24 months after activation of the CI. Details of the figure are otherwise the same as those of Fig. 3

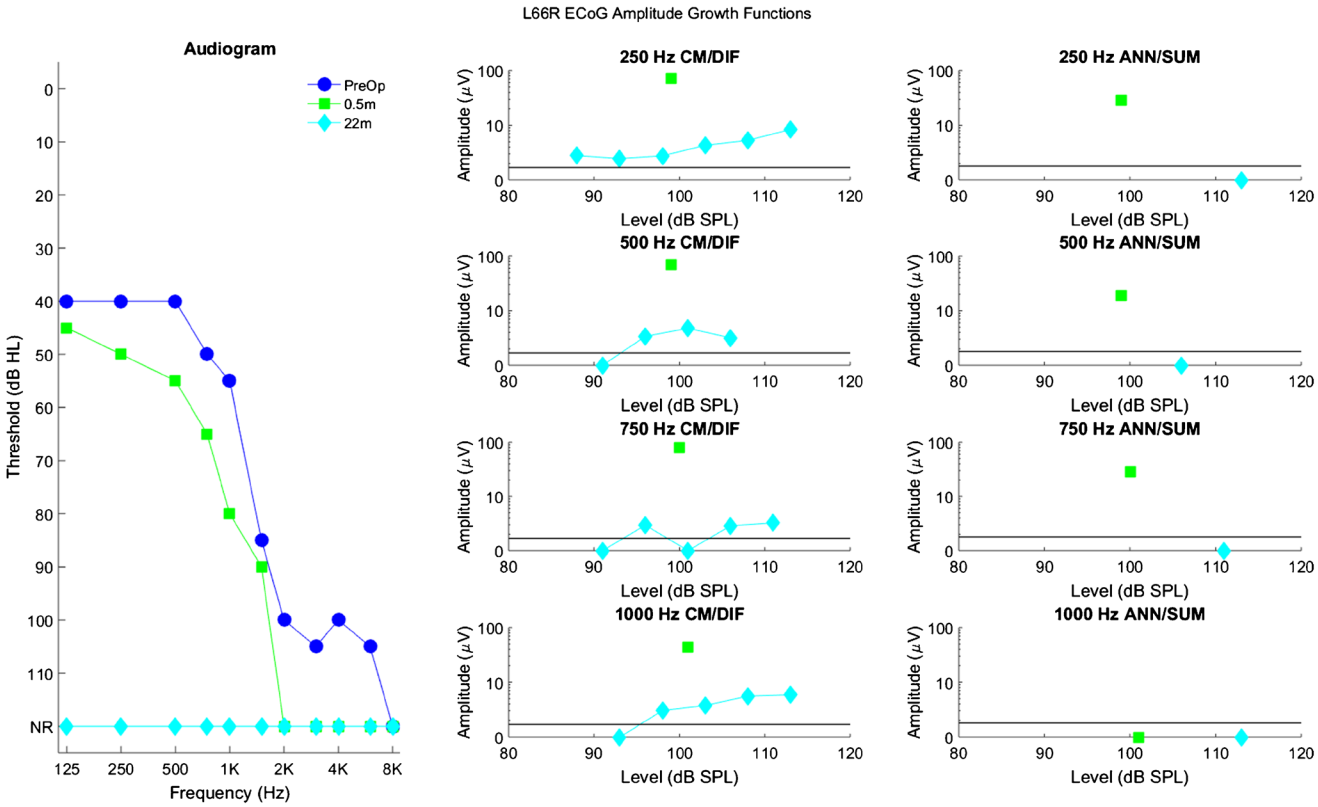

FIG. 8. Longitudinal audiograms and ECoG amplitude growth functions for subject L66R up to 22 months after activation of the CI. Details of the figure are otherwise the same as those of Fig. 3

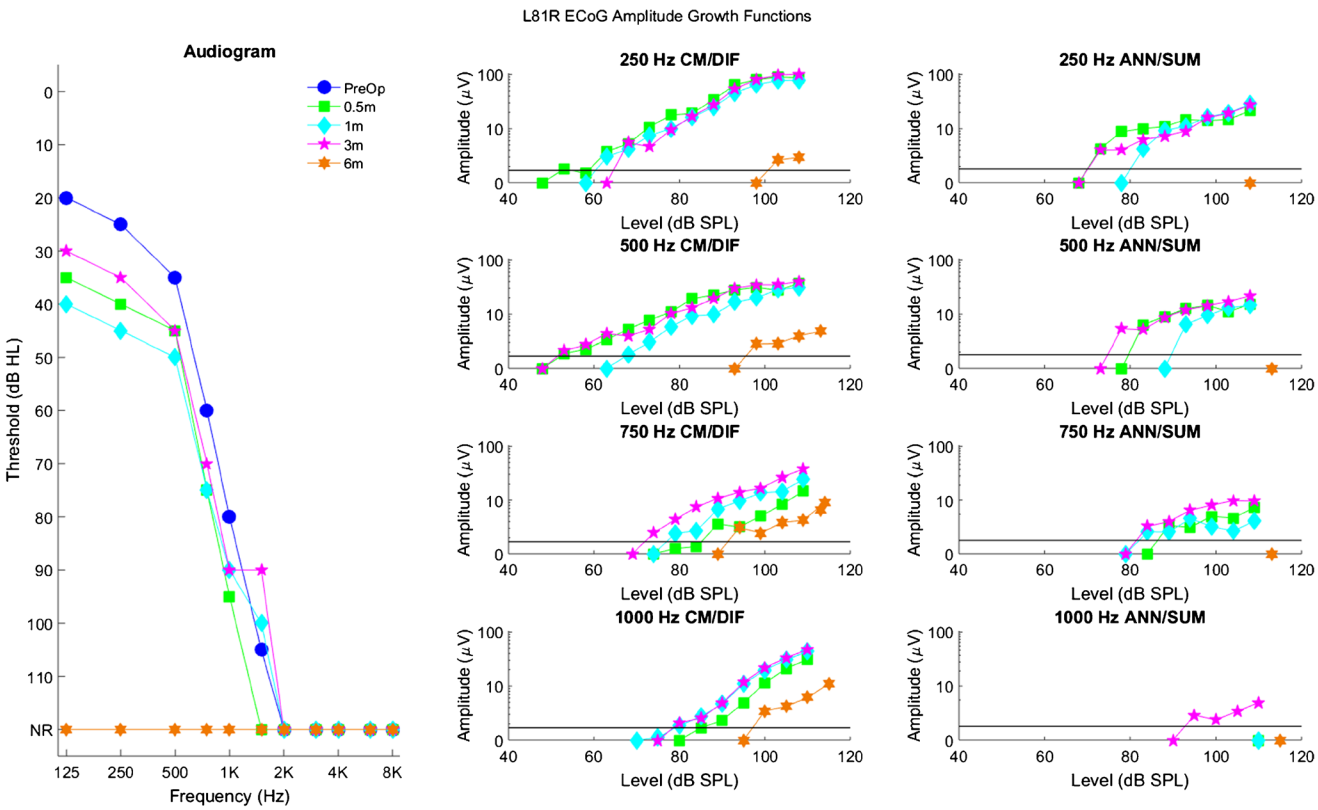

FIG. 9. Longitudinal audiograms and ECoG amplitude growth functions for subject L81R up to 6 months after activation of the CI. Details of the figure are otherwise the same as those of Fig. 3

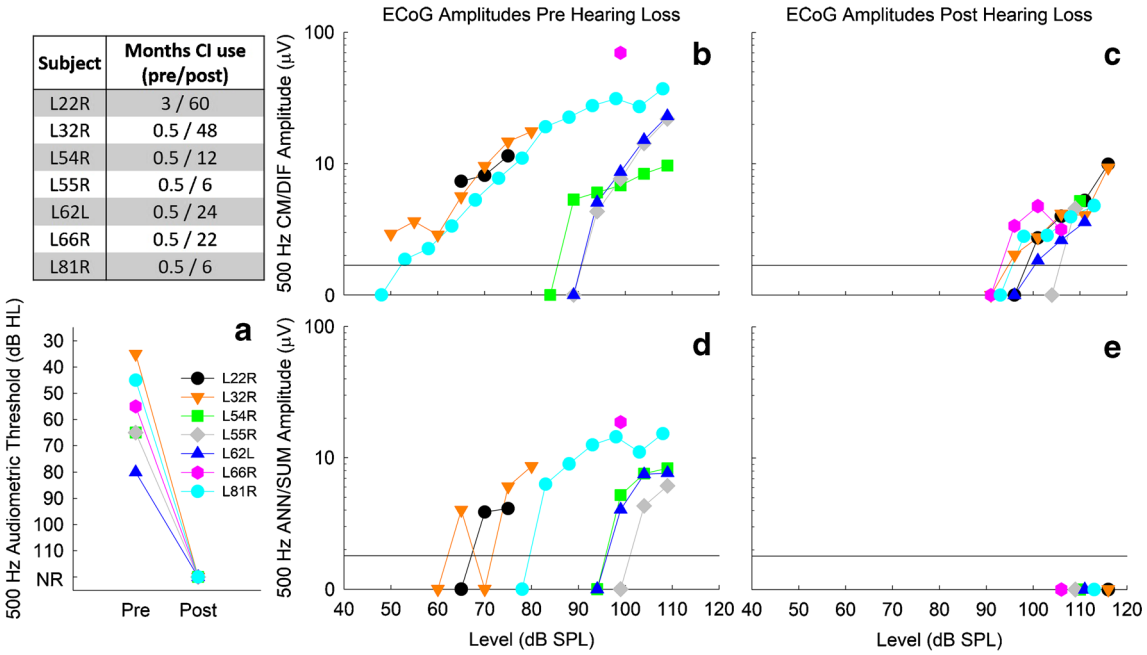

FIG. 10. Summary of audiometric thresholds and ECoG amplitude growth functions for 500 Hz for all subjects at one time before and one time after hearing loss, as shown in the table. Panel A: audiometric threshold at 500 Hz before and after hearing loss. NR signifies no response. B and C: CM/DIF amplitude growth functions before and after total hearing loss. After total loss of hearing, growth functions shift to the right, indicating that higher levels were needed to evoke a CM/DIF response. Panels D and E: ANN/SUM amplitude growth functions before and after total hearing loss. After total loss of hearing, no ANN/SUM responses could be recorded. The black line at 1.73 μV in panels B–E indicates the noise floor

nature of the original dataset used to build the model. Most CM/DIF and ANN/SUM amplitudes are below 20 μV in the original dataset (Fig. 12). However, there are several cases where CM/DIF amplitudes are much higher than 20 μV while the corresponding ANN/SUM amplitudes do not appreciably increase, resulting in a wider prediction interval.

The CM/DIF amplitudes *after hearing loss* (Fig. 10C) were used as inputs to the linear mixed-effects model to form a prediction interval of the expected ANN/SUM amplitude based on the CM/DIF amplitude (Fig. 14). As previously shown in Fig. 10E, there were no recordable ANN/SUM responses after total loss of hearing. However, based on the CM/DIF amplitudes recorded after loss of hearing, the model predicted ANN/SUM amplitudes of 4–5 μV, which is well above the noise floor. While the 95 % prediction intervals do indicate smaller amplitudes below the noise floor (which normally would lead to the 0 μV responses shown in Fig. 10E), it is more likely that amplitudes

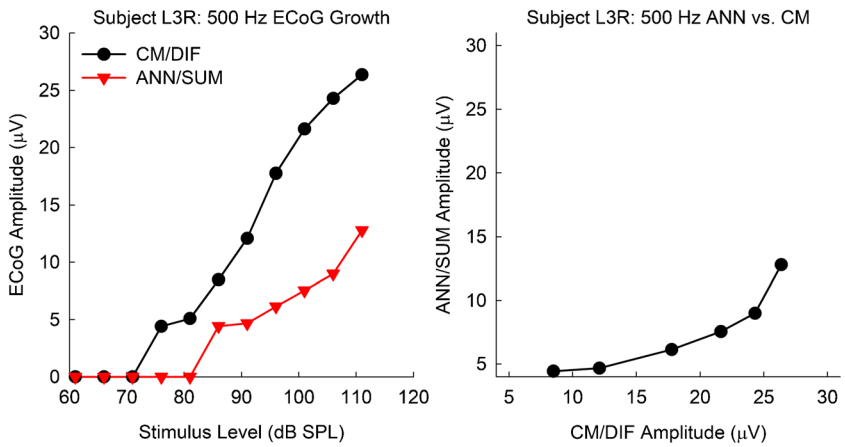

FIG. 11. (Left) Exemplar CM/DIF and ANN/SUM amplitude growth functions in response to a 500-Hz tone burst. (Right) The same data, but with the CM/DIF and the corresponding ANN/SUM plotted against one another

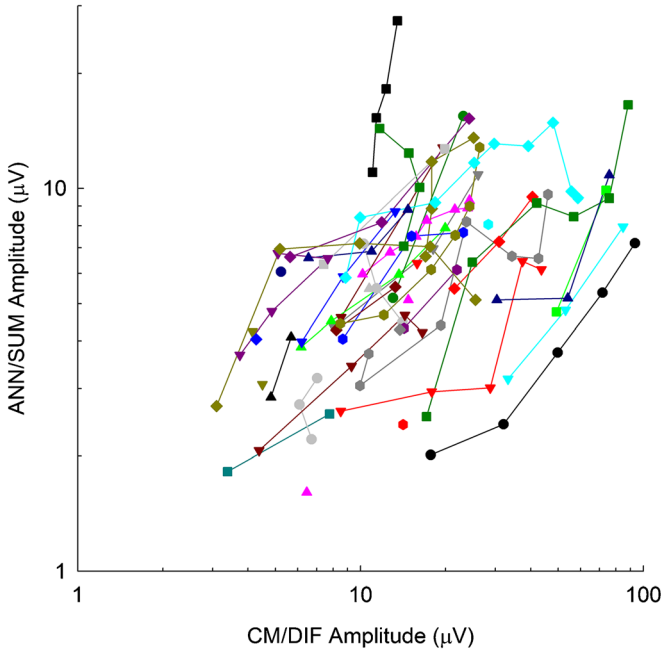

FIG. 12. CM/DIF amplitudes and the corresponding ANN/SUM amplitudes plotted against one another for all 51 subjects

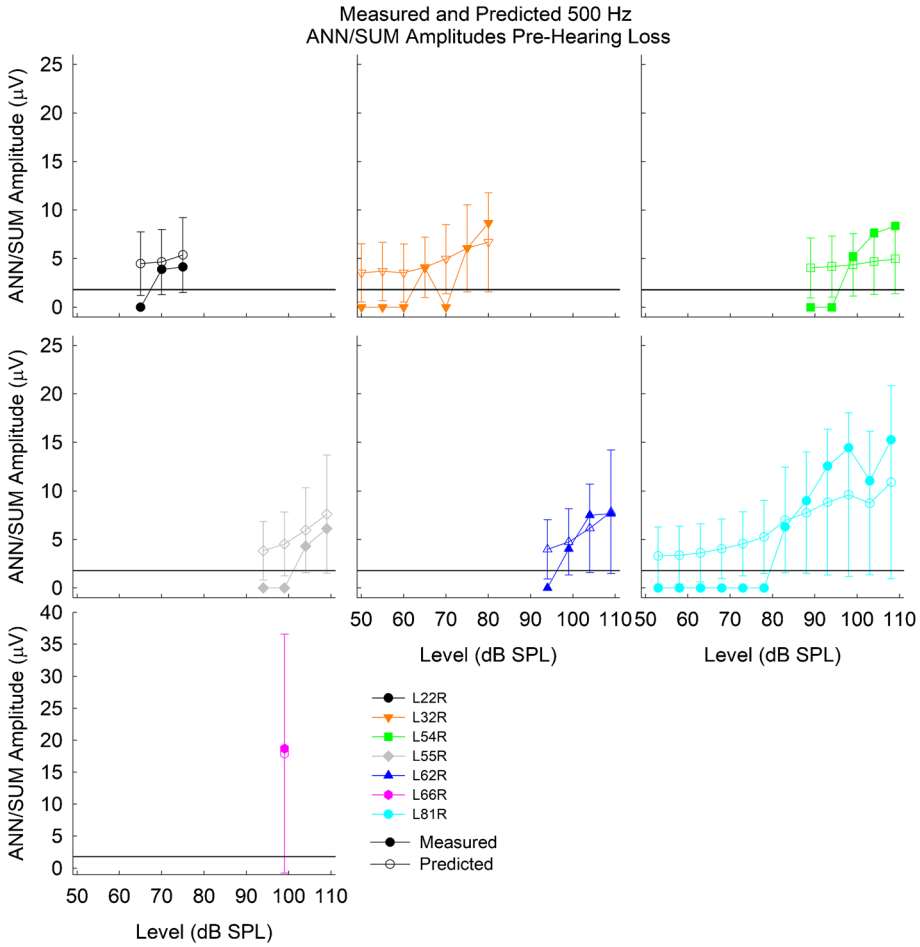

FIG. 13. Predicted and measured ANN/SUM potentials before loss of acoustic hearing. Bars represent the 95 % prediction interval. The horizontal line at 1.73 μV indicates the noise floor

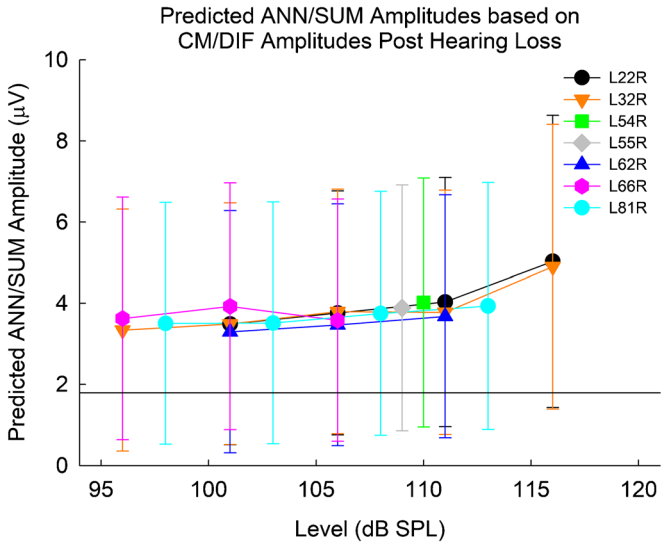

FIG. 14. Predicted ANN/SUM potentials after loss of acoustic hearing for all subjects. Bars represent the 95 % prediction interval. The horizontal line at 1.73 μV indicates the noise floor

should have been above the recording noise floor and therefore present even after total loss of acoustic hearing. Thus, we argue that the noise floor likely did not obscure any true ANN/SUM response after total loss of acoustic hearing.

DISCUSSION

We previously demonstrated that both CM/DIF and ANN/SUM responses decline with partial loss of audiometric hearing (Abbas et al. 2017; Kim et al. 2018). The current study extends our previous findings by emphasizing L24 Hybrid CI users with complete loss of residual hearing. When considering recent studies by Fitzpatrick and colleagues, the current results suggest a synaptic issue (Choudhury et al. 2012; Fitzpatrick et al. 2014; Formeister et al. 2015; Fontenot et al. 2019). Fitzpatrick and colleagues reported intraoperative ECoG measures using a recording electrode placed on the round window prior to cochlear implantation in hundreds of patients. Patients with large CM responses also had measurable ANN responses and/or compound action potentials, reflecting a healthier population of hair cells that could support transmission of information to auditory nerve fibers. Conversely, a small CM reflected a "disconnection" between hair cells and nerve fibers, leading to no audiometric hearing. They reasoned this disconnection could explain why CM thresholds are lower (better) then behavioral thresholds for several patients in their studies. Their results are consistent with the small CMs and no ANNs in our subjects after hearing loss (Figs. 2, 3, 4, 5, 6, 7, 8, and 9). The "disconnection" theory of synaptic involvement implies that despite some viable hair cell function, there is compromised encoding of auditory stimulation to the auditory nerve, leading to lack of audiometric hearing in our subjects.

Since audiometric thresholds are strongly correlated with CM and ANN thresholds (Abbas et al. 2017; Koka et al. 2017; Kim et al. 2018), the elevation in thresholds for all three measures is likely affected by a common mechanism. This mechanism is likely unrelated to hair cell or spiral ganglion neural pathology, as hair cell, neural, pre-synaptic ribbon counts, and post-synaptic receptor counts, are stable after loss of acoustic hearing O'Leary et al. 2013; Tanaka et al. 2014; Reiss et al. 2015; Quesnel et al. 2016). In contrast, Eshraghi et al. (2013) observed outer hair cell loss, but their protocol involved extensive electrode-induced cochlear trauma such that dramatic shifts in both low- and high-frequency hearing were observed. Similarly, ECAP measures reflect the response of the auditory nerve to *electrical* stimulation and could serve as a proxy of neural health. We previously showed that ECAPs remained unchanged before and after hearing loss in EAS CI patients (Scheperle et al. 2017). Many of these patients had partial loss of acoustic hearing, while the current study focused on total loss. Unfortunately, the retrospective nature of the current study, as well as limited subject availability, did not allow for proper comparisons of ECAPs before and after hearing loss. Only subjects L32R, L55R, and L81R have ECAP data before and after hearing loss. ECAP amplitudes and thresholds for L32R and L55R were stable after total loss of acoustic hearing while L81R presented with reduced ECAP amplitudes and stable ECAP thresholds at the apical electrodes. L32R and L55R ECAP

results are consistent with our previous report (Scheperle et al. 2017) and seem to rule out a neural involvement. As a caveat, the L24 electrode array is inserted to a 220- to 270-degree depth (Briggs et al. 2006; Lenarz et al. 2006; Driscoll et al. 2011), corresponding to the 1500–2000 Hz place in the cochlea (Stakhovskaya et al. 2007). Thus, ECAP measures reflect neural activity from the cochlear base and cannot definitively rule out neural involvement at the cochlear apex where low-frequency hearing loss occurs. However, histological studies have shown stable neural counts in cochlear regions both adjacent and apical to the electrode in cases of delayed hearing loss (O'Leary et al. 2013; Tanaka et al. 2014; Reiss et al. 2015; Quesnel et al. 2016).

A recent theory of delayed hearing loss involves an interaction of tissue response and cochlear mechanics (Foggia et al. 2019); this theory could account for the reduced ECoG responses. A tissue response consisting of fibrosis/osteoneogenesis has been observed at the cochleostomy site (Tanaka et al. 2014) and the lower basal turn where the electrode resides (O'Leary et al. 2013; Quesnel et al. 2016), but not in the apical turns (O'Leary et al. 2013; Quesnel et al. 2016). In their guinea pig model, O'Leary et al. (2013) showed that fibrosis and osteoneogenesis were both correlated with Auditory Brainstem Response (ABR) threshold shifts at 8 kHz, a region apical relative to the electrode array. These correlations were weaker or nonsignificant at frequency regions where the electrode resided (16, 24, 32 kHz) and a region very apical (2 kHz). On the contrary, Tanaka et al. (2014) did not see correlations between fibrosis and low/high-frequency ABR thresholds shifts (1, 6, 16 kHz) in their guinea pig model. However, in addition to their smaller sample size, their tissue measures were done at the cochleostomy site rather than the electrode region. Despite the lack of a tissue response at the apical turn in both human and animal CI models (O'Leary et al. 2013; Tanaka et al. 2014; Quesnel et al. 2016), computational simulations suggest that the tissue response at the basal turn may compromise cochlear mechanics and account for apical low-frequency hearing loss (Choi and Oghalai 2005). This loss of cochlear mechanics could account for the reduced ECoG amplitudes, manifesting itself as reduced hair cell function and synaptic input and leading to loss of audiometric hearing.

The presence of fibrosis could account for elevated electrode impedances in EAS patients with loss of hearing seen in our clinic (Scheperle et al. 2017) and elsewhere (Choi et al. 2017). Electrode impedance reflects the intracochlear environment and the electrode/electrolyte interface (Dymond 1976; Tykocinski et al. 2005). Subjects L22R, L32R, and L81R demonstrated elevated electrode impedances at the time of their sudden hearing loss, and were prescribed prednisone to reduce possible inflammatory responses associated with sudden hearing loss (Rauch et al. 2011). L22R and L32R demonstrated temporary improvements in audiometric hearing (Figs. 2 and 3), and while L81R did not see improvements in audiometric hearing, she experienced a temporary reduction in electrode impedances. L81R was also explanted due to device failure (presumably soft failure) and reimplanted with a full-length 20-mm electrode array. During the revision surgery, her surgeon (author MRH) noted extensive fibrosis/ossification in the scala tympani, forcing him to leave several electrodes extracochlear. These observations are consistent with histological data (O'Leary et al. 2013; Tanaka et al. 2014; Quesnel et al. 2016), and computational modeling (Choi and Oghalai 2005), suggesting compromised cochlear mechanics due to intracochlear fibrosis. We are currently conducting complex impedance measures and analyses that could provide further insight into intracochlear fibrotic reactions in our EAS population (Yang et al. 2019).

Based on their histological measures, Reiss and colleagues (Tanaka et al. 2014; Reiss et al. 2015) suggested trauma to the lateral wall and stria vascularis contributes to loss of hearing in the high-frequency cochlear regions occupied by the electrode array. This theory cannot be addressed directly in our human CI patients. Additionally, clinically speaking, the high-frequency hearing present preoperatively in our EAS patients is generally too severe to provide functional use.

There are a few caveats regarding the ANN data. While the lack of ANN responses may partly be due to a noise floor issue, our statistical modeling suggests that noise floor is likely not a major confound (Figs. 12, 13, and 14). Secondly, summation of rarefaction and condensation responses does not completely eliminate CM and isolate ANN responses, as ANN responses are likely contaminated by some CM responses, especially at stimulation levels greater than 30–40 dB re: CM response thresholds (Forgues et al. 2014). Lastly, neural responses are susceptible to adaptation (Mouney et al. 1978). We previously showed that both CM/DIF and ANN/SUM potentials were susceptible to adaptation, though the ANN/SUM was more susceptible than the CM/DIF (Abbas et al. 2017). Thus, ANNs collected prior to hearing loss in the current study may be contaminated by some hair cell contributions, particularly at high stimulus levels. These caveats also apply to the data from the 51 subjects used in the model and can affect modeling results. However, the contamination of the ANN by the CM seems more problematic at high stimulus levels relative to the CM threshold (Forgues et al. 2014). For most subjects, we are not able to

stimulate at such high levels without loudness discomfort issues, thus the contamination, while present, may not be as problematic.

A fast Fourier transform (FFT) is generally used to transpose the time domain ECoG waveform data into the frequency domain, which allows identification of the peak amplitude at the fundamental frequency of the stimulus and subsequent harmonics (e.g., Koka et al. 2017; Fontenot et al. 2019; Tejani et al. 2019). This is a more precise method of quantifying the strength of the CM and ANN responses. ECoG amplitudes were measured in the time domain for the current study because the current study was partly a retrospective review of data from Kim et al. (2018), where a short recording buffer prevented high-resolution FFT analysis. For other patients seen under protocols developed by Abbas et al. (2017) and Tejani et al. (2019), longer recording buffers allowed for high-resolution FFT analysis but were still analyzed in the time waveform to maintain consistency with Kim et al. (2018). However, in the subjects that we could measure FFT responses, the presence or absence of FFT responses was consistent with the results based on peak measures reported here. Additionally, since neural responses are susceptible to adaptation, one can pick peaks from a single cycle of the unadapted portion of the time waveform (e.g., subject L32R, Fig. 2).

Minimizing hearing loss and cochlear trauma is the ideal outcome of CI surgeries. When patients experience partial/total loss of acoustic hearing, sound processors are reprogrammed to provide electrical stimulation of low-frequency bands in addition to high-frequency bands. However, compressing more frequency information into a shorter electrode array compared to a longer conventional electrode array potentially decreases speech recognition (Başkent and Shannon 2004, 2005) due to disruptions in tonotopic matching (Landsberger et al. 2015). Despite the compressed frequency information, Hybrid CI patients with profound/total loss of acoustic hearing still show significant improvements in speech understanding compared to pre-operative status, though greater speech recognition benefits are seen with better hearing preservation (Gantz et al. 2016; Roland et al. 2016; Dunn et al. 2020). Thus, investigating the possible causes of post-implant cochlear trauma and/or hearing loss remains an important topic in the CI literature to optimize EAS success.

The current study further demonstrates clinical utility of ECoG in investigating hair cell and neural function in EAS CI users. The reduced CM responses in addition to the lack of ANN responses, in conjunction with previous electrophysiological (Scheperle et al. 2017; Fontenot et al. 2019) and histological data (O'Leary et al. 2013; Tanaka et al. 2014; Quesnel et al. 2016), support reduced synaptic input due to a reduction in hair cell function. The exact pathophysiology is a multifaceted issue (e.g., fibrosis, bone growth, stria trauma, synaptopathy), but if causes of post-implant hearing loss can be identified, it will guide future audiological and/or medical interventions.

Funding National Institutes of Health/National Institute on Deafness and Other Communicative Disorders P50 DC 00242 (PI: Gantz)

COMPLIANCE WITH ETHICAL STANDARDS

Conflict of Interest BJG is a consultant for Cochlear Ltd. MRH is co-founder and Chief Medical Officer for iotaMotion, Inc. VDT is a consultant for iotaMotion, Inc. All other authors declare that they have no conflict of interest.

Publisher's Note Springer Nature remains neutral with regard to jurisdictional claims in published maps and institutional affiliations.

REFERENCES

ABBAS PJ, TEJANI VD, SCHEPERLE RA, BROWN CJ (2017) Using neural response telemetry to monitor physiological responses to acoustic stimulation in hybrid cochlear implant users. Ear Hear. 38(4):409–425. https://doi.org/10.1097/AUD.0000000000000400

ADUNKA OF, PILLSBURY HC, BUCHMAN CA (2010) Minimizing intracochlear trauma during cochlear implantation. Adv Otorhinolaryngol. 67:96–107. https://doi.org/10.1159/000262601

ARAN J-M, CHARLET DE SAUVAGE R (1976) Clinical value of cochlear microphonic recordings. In: Ruben RJ, Elberling C, Salomon G (eds) Electrocochleography. University Park Press, Baltimore, MD, p 55e65

BAŞKENT D, SHANNON RV (2004) Frequency-place compression and expansion in cochlear implant listeners. J Acoust Soc Am. 116(5):3130–3140. https://doi.org/10.1121/1.1804627

BAŞKENT D, SHANNON RV (2005) Interactions between cochlear implant electrode insertion depth and frequency-place mapping. J Acoust Soc Am. 117(3 Pt 1):1405–1416. https://doi.org/10.1121/1.1856273

BRIGGS RJ, TYKOCINSKI M, XU J, RISI F, SVEHLA M, COWAN R, STOVER T, ERFURT P, LENARZ T (2006) Comparison of round window and cochleostomy approaches with a prototype hearing preservation electrode. Audiol. Neuro. Otol. 42e48. https://doi.org/10.1159/000095613

CHOI C-H, OGHALAI JS (2005) Predicting the effect of post-implant cochlear fibrosis on residual hearing. Hear Res. 205(1-2):193–200. https://doi.org/10.1016/j.heares.2005.03.018

CHOI J, PAYNE MR, CAMPBELL LJ, BESTER CW, NEWBOLD C, EASTWOOD H, O'LEARY SJ (2017) Electrode impedance fluctuations as a biomarker for inner ear pathology after cochlear implantation. Otol Neurotol. 38(10):1433–1439. https://doi.org/10.1097/MAO.0000000000001589

Choudhury B, Fitzpatrick DC, Buchman CA, Wei BP, Dillon MT, He S, Adunka OF (2012) Intraoperative round window recordings to acoustic stimuli from cochlear implant patients. Otol Neurotol. 33(9):1507–1515. https://doi.org/10.1097/MAO.0b013e31826dbc80

Driscoll CL, Carlson ML, Fama AF, Lane JI (2011) Evaluation of the Hybrid-L24 electrode using microcomputed tomography. Laryngoscope 121(7):e1508–e1516. https://doi.org/10.1002/lary.21837

Dunn CC, Oleson J, Parkinson A, Hansen MR, Gantz BJ (2020) Nucleus hybrid S12: multicenter clinical trial results. Laryngoscope. 130(10):E548–E558. https://doi.org/10.1002/lary.28628

Dymond AM (1976) Characteristics of the metal-tissue interface of stimulation electrodes. IEEE Trans Biomed Eng. 23(4):274–280. https://doi.org/10.1109/tbme.1976.324585

Eggermont JJ (2017) Ups and Downs in 75 Years of Electrocochleography. Front Syst Neurosci. 11:2. https://doi.org/10.3389/fnsys.2017.00002

Eshraghi AA, Gupta C, Van De Water TR, Bohorquez JE, Garnham C, Bas E, Talamo VM (2013) Molecular mechanisms involved in cochlear implantation trauma and the protection of hearing and auditory sensory cells by inhibition of c-Jun-N-terminal kinase signaling. Laryngoscope. 123 Suppl 1:S1–14. https://doi.org/10.1002/lary.23902

Fitzpatrick DC, Campbell AP, Choudhury B, Dillon MT, Forgues M, Buchman CA, Adunka OF (2014) Round window electrocochleography just before cochlear implantation: relationship to word recognition outcomes in adults. Otol Neurotol 35(1):64–71. https://doi.org/10.1097/MAO.0000000000000219

Foggia MJ, Quevedo RV, Hansen MR (2019) Intracochlear fibrosis and the foreign body response to cochlear implant biomaterials. Laryngoscope Investig Otolaryngol 4(6):678–683. https://doi.org/10.1002/lio2.329

Fontenot TE, Giardina CK, Dillon M, Rooth MA, Teagle HF, Park LR, Brown KD, Adunka OF, Buchman CA, Pillsbury HC, Fitzpatrick DC (2019) Residual cochlear function in adults and children receiving cochlear implants: correlations with speech perception outcomes. Ear Hear. 40(3):577–591. https://doi.org/10.1097/AUD.0000000000000630

Forgues M, Koehn HA, Dunnon AK, Pulver SH, Buchman CA, Adunka OF, Fitzpatrick DC (2014) Distinguishing hair cell from neural potentials recorded at the round window. J Neurophysiol. 111(3):580–593. https://doi.org/10.1152/jn.00446.2013

Formeister E, McClellan JH, Merwin WH 3rd, Iseli CE, Calloway NH, Teagle HF, Buchman CA, Adunka OF, Fitzpatrick DC (2015) Intraoperative round window electrocochleography and speech perception outcomes in pediatric cochlear implant recipients. Ear Hear. 36(2):249–260. https://doi.org/10.1097/AUD.0000000000000106

Gantz BJ, Dunn CC, Oleson J, Hansen MR, Parkinson A, Turner C (2016) Multicenter clinical trial of the Nucleus hybrid S8 cochlear implant: Final outcomes. Laryngoscope. 126:962–973. https://doi.org/10.1002/lary.25572

Gantz BJ, Dunn CC, Oleson J, Hansen MR (2018) Acoustic plus electric speech processing: long-term results. Laryngoscope. 128(2):473–481. https://doi.org/10.1002/lary.26669

Helbig S, Van de Heyning P, Kiefer J, Baumann U, Kleine-Punte A, Brockmeier H, Anderson I, Gstoettner W (2011) Combined electric acoustic stimulation with the PULSARCI^{100} implant system using the FLEX^{EAS} electrode array. Acta Otolaryngol. 131(6):585–595. https://doi.org/10.3109/00016489.2010.544327

Henry KR (1995) Auditory nerve neurophonic recorded from the round window of the Mongolian gerbil. Hear Res. 90(1-2):176–184. https://doi.org/10.1016/0378-5955(95)00162-6

Kim JS, Tejani VD, Abbas PJ, Brown CJ (2018) Postoperative electrocochleography from hybrid cochlear implant users: an alternative analysis procedure. Hear Res. 370:304–315. https://doi.org/10.1016/j.heares.2018.10.016

Koka K, Saoji AA, Litvak LM (2017) Electrocochleography in cochlear implant recipients with residual hearing: comparison with audiometric thresholds. Ear Hear. 38(3):e161–e167. https://doi.org/10.1097/AUD.0000000000000385

Kopelovich JC, Reiss LA, Etler CP, Xu L, Bertroche JT, Gantz BJ, Hansen MR (2015) Hearing loss after activation of hearing preservation cochlear implants might be related to afferent cochlear innervation injury. Otol Neurotol. 36(6):1035–1044. https://doi.org/10.1097/MAO.0000000000000754

Landsberger DM, Svrakic M, Roland JT Jr, Svirsky M (2015) The relationship between insertion angles, default frequency allocations, and spiral ganglion place pitch in cochlear implants. Ear Hear. 36(5):e207–e213. https://doi.org/10.1097/AUD.0000000000000163

Lenarz T, Stover T, Buechner A, Paasche G, Briggs R, Risi F, Pesch J, Battmer RD (2006) Temporal bone results and hearing preservation with a new straight electrode. Audiol. Neuro. Otol. 11 (Suppl. 1), 34e41. https://doi.org/10.1159/000095612

Lenarz T, James C, Cuda D, Fitzgerald O'Connor A, Frachet B, Frijns JH, Klenzner T, Laszig R, Manrique M, Marx M, Merkus P, Mylanus EA, Offeciers E, Pesch J, Ramos-Macias A, Robier A, Sterkers O, Uziel A (2013) European multi-centre study of the Nucleus Hybrid L24 cochlear implant. Int J Audiol. 52(12):838–848. https://doi.org/10.3109/14992027.2013.802032

Li Q, Lu T, Zhang C, Hansen MR, Li S (2020) Electrical stimulation induces synaptic changes in the peripheral auditory system. J Comp Neurol. 528(6):893–905. https://doi.org/10.1002/cne.24802

Lichtenhan JT, Cooper NP, Guinan JJ Jr (2013) A new auditory threshold estimation technique for low frequencies: Proof of concept. Ear Hear. 34(1):42–51. https://doi.org/10.1097/AUD.0b013e31825f9bd3

Mouney DF, Berlin CI, Cullen JK Jr, Hughes LF (1978) Changes in human eighth nerve action potential as a function of stimulation rate. Arch Otolaryngol. 104(10):551–554. https://doi.org/10.1001/archotol.1978.00790100005001

O'Leary SJ, Monksfield P, Kel G, Connolly T, Souter MA, Chang A, Marovic P, O'Leary JS, Richardson R, Eastwood H (2013) Relations between cochlear histopathology and hearing loss in experimental cochlear implantation. Hear Res. 298:27–35. https://doi.org/10.1016/j.heares.2013.01.012

Pappa AK, Hutson KA, Scott WC, Wilson JD, Fox KE, Masood MM, Giardina CK, Pulver SH, Grana GD, Askew C, Fitzpatrick DC (2019) Hair cell and neural contributions to the cochlear summating potential. J Neurophysiol. 121(6):2163–2180. https://doi.org/10.1152/jn.00006.2019

Pillsbury HC 3rd, Dillon MT, Buchman CA, Staecker H, Prentiss SM, Ruckenstein MJ, Bigelow DC, Telischi FF, Martinez DM, Runge CL, Friedland DR, Blevins NH, Larky JB, Alexiades G, Kaylie DM, Roland PS, Miyamoto RT, Backous DD, Warren FM, El-Kashlan HK, Slager HK, Reyes C, Racey AI, Adunka OF (2018) Multicenter US clinical trial with an Electric-Acoustic Stimulation (EAS) system in adults: final outcomes. Otol Neurotol. 39(3):299–305. https://doi.org/10.1097/MAO.0000000000001691

Quesnel AM, Nakajima HH, Rosowski JJ, Hansen MR, Gantz BJ, Nadol JB Jr (2016) Delayed loss of hearing after hearing preservation cochlear implantation: Human temporal bone pathology and implications for etiology. Hear Res. 333:225–234. https://doi.org/10.1016/j.heares.2015.08.018

Rauch SD, Halpin CF, Antonelli PJ, Babu S, Carey JP, Gantz BJ, Goebel JA, Hammerschlag PE, Harris JP, Isaacson B, Lee D, Linstrom CJ, Parnes LS, Shi H, Slattery WH, Telian SA, Vrabec JT, Reda DJ (2011) Oral vs intratympanic corticosteroid therapy for idiopathic sudden sensorineural hearing loss: a randomized

trial. JAMA. 305(20):2071–2079. https://doi.org/10.1001/jama.2011.679

REISS LA, STARK G, NGUYEN-HUYNH AT, SPEAR KA, ZHANG H, TANAKA C, LI H (2015) Morphological correlates of hearing loss after cochlear implantation and electro-acoustic stimulation in a hearing-impaired Guinea pig model. Hear Res. 327:163–174. https://doi.org/10.1016/j.heares.2015.06.007

ROLAND JT JR, GANTZ BJ, WALTZMAN SB, PARKINSON AJ, MULTICENTER CLINICAL TRIAL GROUP (2016) United States multicenter clinical trial of the cochlear nucleus hybrid implant system. Laryngoscope. 126(1):175–181. https://doi.org/10.1002/lary.25451

ROLAND JT JR, GANTZ BJ, WALTZMAN SB, PARKINSON AJ (2018) Long-term outcomes of cochlear implantation in patients with high-frequency hearing loss. Laryngoscope. 128(8):1939–1945. https://doi.org/10.1002/lary.27073

SCHEPERLE RA, TEJANI VD, OMTVEDT JK, BROWN CJ, ABBAS PJ, HANSEN MR, GANTZ BJ, OLESON JJ, OZANNE MV (2017) Delayed changes in auditory status in cochlear implant users with preserved acoustic hearing. Hear Res. 350:45–57. https://doi.org/10.1016/j.heares.2017.04.005

STAKHOVSKAYA O, SRIDHAR D, BONHAM BH, LEAKE PA (2007) Frequency map for the human cochlear spiral ganglion: implications for cochlear implants. J Assoc Res Otolaryngol. 8(2):220–233. https://doi.org/10.1007/s10162-007-0076-9

TANAKA C, NGUYEN-HUYNH A, LOERA K, STARK G, REISS L (2014) Factors associated with hearing loss in a normal-hearing guinea pig model of Hybrid cochlear implants. Hear Res. 316:82–93. https://doi.org/10.1016/j.heares.2014.07.011

TEJANI VD, ABBAS PJ, BROWN CJ, WOO J (2019) An improved method of obtaining electrocochleography recordings from Nucleus Hybrid cochlear implant users. Hear Res. 373:113–120. https://doi.org/10.1016/j.heares.2019.01.002

TYKOCINSKI M, COHEN LT, COWAN RS (2005) Measurement and analysis of access resistance and polarization impedance in cochlear implant recipients. Otol Neurotol. 26(5):948–956. https://doi.org/10.1097/01.mao.0000185056.99888.f3

VAN ABEL KM, DUNN CC, SLADEN DP, OLESON JJ, BEATTY CW, NEFF BA, HANSEN M, GANTZ BJ, DRISCOLL CL (2015) Hearing preservation among patients undergoing cochlear implantation. Otol Neurotol 36(3):416–421. https://doi.org/10.1097/mao.0000000000000703

YANG H, TEJANI VD, KIM J-S, ABBAS PJ, BROWN CJ, WOO J (2019) Localized impedance changes with delayed-onset hearing loss in hybrid cochlear implant users. in: conference on implantable auditory prostheses, lake Tahoe, CA, July 2019